Carbon Letters (2023) 33:1811–1817
https://doi.org/10.1007/s42823-023-00560-w

Online ISSN 2233-4998
Print ISSN 1976-4251

ORIGINAL ARTICLE

A graphene-based highly sensitive aptasensor for the detection of lung cancer marker CA125

Junnan Chen[1] · Lingmin Yu[2] · Wenzhen Xu[1] · Tao Lin[1] · Sicong Jiang[3] · Caijin Jin[1]

Received: 11 April 2023 / Revised: 29 May 2023 / Accepted: 14 June 2023 / Published online: 26 June 2023

Abstract

Graphene-based sensors have emerged as significant tools for biosensing applications due to their unique electrical, mechanical, and thermal properties. In this study, we have developed an innovative and sensitive aptasensor based on the surface-modified graphene for the detection of lung cancer biomarker CA125. The sensor leverages the combination of graphene surface and gold nanoparticles (AuNPs) electrodeposition to achieve a high level of sensitivity and selectivity for the biomarker detection. A noticeable decrease in electron transfer resistance was observed upon the AuNPs deposition, demonstrating the enhancement of electrochemical performance. Our experimental findings showed a strong linear relationship between the sensor response and CA125 concentrations, ranging from 0.2 to 15.0 ng/mL, with a detection limit of 0.085 ng/mL. This study presents a novel approach to lung cancer detection, surpassing the traditional methods in terms of invasiveness, cost, and accuracy. The results from this work could pave the way for the development of graphene-based sensors in various other biosensing applications.

Keywords Lung cancer · CA125 · Graphene · Electrochemical sensor · Aptasensor

1 Introduction

Lung cancer is a leading cause of mortality worldwide, with an increasing prevalence observed in the recent decades due to various factors, including lifestyle habits and environmental conditions [1, 2]. As with many types of cancer, early detection is key in lung cancer to ensure more successful treatment outcomes and improve patient survival rates [3]. Despite advances in medical technology, current detection methods for lung cancer, such as biopsy and imaging techniques, are invasive, costly, and often not sufficiently accurate for early-stage diagnosis [4, 5].

✉ Caijin Jin
18370608520@163.com

Junnan Chen
xiongwaikechenjunnan@syqw3.wecom.work

[1] Department of Cardio-Thoracic Surgery, Sanmen People's Hospital, Taizhou, Zhejiang, China

[2] Sanmen County Medical Emergency Center, 171 Renmin Road, Sanmen County, Taizhou, Zhejiang, China

[3] Division of Thoracic and Endocrine Surgery, University Hospitals and University of Geneva, 1211 Geneva 4, Switzerland

Cancer antigen 125 (CA125) has been identified as a valuable biomarker for lung cancer, especially during the early stages of the disease. Elevated levels of CA125 in serum have been strongly correlated with the presence of lung cancer, making it an attractive target for diagnostic assays [6, 7]. The development of highly sensitive and selective detection methods for CA125 is critical for enhancing the accuracy of lung cancer diagnosis and enabling timely treatment interventions [8, 9]. Determining the concentration of CA125 is of significant clinical relevance, as it is a biomarker associated with various cancers, including ovarian, endometrial, peritoneal, and lung cancer. Recent studies have increasingly highlighted its importance. For instance, Charkhchi et al. [10] emphasized the role of CA125 in the early detection of ovarian cancer, while Wang et al. [11] underscored its potential as a prognostic indicator in lung cancer patients. Moreover, a recent meta-analysis by Njoku et al. [12] reinforced the significance of CA125 levels in predicting overall survival and treatment response in endometrial cancer. These studies underscore the urgent need for sensitive, accurate, and user-friendly methods of CA125 determination, which our novel aptasensor aims to fulfill.

Aptasensors, which are based on the specific recognition of target molecules by aptamers, have emerged as a

promising alternative to traditional diagnostic methods [13]. Aptamers are single-stranded DNA or RNA molecules that can bind to their target molecules, such as proteins or small molecules, with high affinity and selectivity [14, 15]. Aptamers offer several advantages over antibodies, including ease of synthesis, low cost, and superior stability under various conditions. These characteristics make aptamers ideal candidates for the development of highly sensitive and selective biosensors for disease diagnosis [16].

Graphene, a single-atom-thick layer of carbon atoms arranged in a two-dimensional honeycomb lattice, has garnered significant attention in recent years due to its unique electronic, mechanical, and thermal properties [17]. Owing to its high surface area, excellent electronic conductivity, and biocompatibility, graphene has been extensively employed in the fabrication of various biosensors, including aptasensors [14]. The large surface area of graphene allows for the immobilization of a high density of aptamers, leading to enhanced sensitivity and signal amplification [18, 19]. Moreover, graphene's biocompatibility makes it suitable for biological applications, such as the detection of cancer biomarkers in complex biological samples [20]. Graphene-based sensors have demonstrated significant potential for biosensing applications due to their unique electrical, mechanical, and thermal properties. Building on this, our study introduces a novel approach, which employs a surface-modified graphene electrode coupled with gold nanoparticle (AuNP) electrodeposition. This innovative design offers enhanced sensitivity and selectivity for the detection of the lung cancer biomarker, CA125. The incorporation of AuNPs enhances the electron transfer rate, making our sensor a significant step forward in biosensing technology.

Despite its many advantages, the hydrophobic nature of pristine graphene poses challenges for its application in biosensing. To overcome this limitation, various surface modification techniques have been developed to improve the hydrophilicity, stability, and biocompatibility of graphene. These modifications not only enhance the interaction between graphene and biomolecules but also facilitate the immobilization of aptamers or antibodies on its surface. In this study, we aimed to develop a highly sensitive and selective graphene-based aptasensor for the detection of the lung cancer biomarker CA125. Graphene was synthesized using a chemical reduction method and subsequently modified to exhibit enhanced hydrophilicity and stability through surface modification techniques. Anti-CA125 antibodies were then immobilized onto the surface of the modified graphene, constructing an aptasensor capable of recognizing and binding to CA125 with high specificity. We assessed the performance of the aptasensor in terms of sensitivity, selectivity, and linear response within the physiologically relevant concentration range of CA125.

2 Experimental

2.1 Materials

All utilized chemicals were of analytical grade and were not subjected to additional purification. The anti-CA125 DNA aptamer (5′-NH2-TTATCGTACGACAGTCATCCTACA C-3′) and its corresponding complementary DNA strand (c-DNA, 5′-GTGTAGGATGAAAAAAGGGTTGGGCGG GATGGGT-3′) were procured from Bioengineering Co., Ltd. 6-Methoxy-1-hexanol (MCH) was acquired from Sigma. Chemicals, such as chloroauric acid, potassium ferricyanide, and potassium ferrocyanide, were obtained from Aladdin Chemical Reagent Shanghai Co., Ltd. Graphene oxide was sourced from Macklin Chemical Reagent Co., Ltd.

2.2 SPE fabrication

Initially, screen-printing templates with different shapes were designed according to the requirements for the conductive silver layer and the conductive carbon layer. A custom-made screen-printing apparatus was then used to print the conductive silver paste onto the polycarbonate printed circuit board using screen-printing technology. After allowing the silver paste to dry in an oven, a conductive carbon paste was printed on the working electrode and counter electrode over the conductive silver layer, followed by drying in an oven. Subsequently, a 1:1 volume ratio mixture of modified acrylic ester A and B adhesive was coated onto the electrode surface. Finally, the SPE was prepared by allowing it to dry under ambient conditions. The detailed steps for preparing the SPE are as follows: in the first step, 0.050 g of graphene was weighed and added to an appropriate amount of carbon paste diluent, followed by ultrasonic dissolution in an ultrasonic cleaner. Then, 2.500 g of conductive carbon paste was added and stirred uniformly to obtain a graphene conductive carbon paste. In the second step, the conductive silver paste was printed onto the PC substrate surface and dried in a 90 °C oven for 30 min. Subsequently, the prepared graphene conductive carbon paste was printed and dried in a 90 °C oven for another 30 min. Finally, an insulating layer was applied, and the electrode was allowed to dry at room temperature for 30 min. The graphene was electrochemically reduced in a pH 7.0 PBS solution (degassed with nitrogen) at a potential range of − 1.8 V to 0 V.

2.3 Preparation of aptamer sensors

The SPE is placed in 0.1 M PBS and subjected to cyclic voltammetry (CV) scanning within a potential range of − 0.5

to 1.5 V for 10 cycles. The SPE is then immersed in 1 mM $HAuCl_4$ and conducted by CV scans. The CV scan is conducted at a potential range of − 1.5 to 1 V, resulting in the Au modification (denoted as A/E). After washing the A/E with water and allowing it to dry at room temperature, 5 µL of 1 µM CA125-aptamer solution is added to the A/E and incubated for 12 h. Then electrode is rinsed with PBS to remove any unbound aptamers, yielding A/A/E. Then, 5 µL of 10.0 nM MCH solution is applied to the A/A/E surface for 10 min to block any remaining vacant sites (denoted as M/A/A/E). Subsequently, the M/A/A/E surface is thoroughly rinsed with PBS to eliminate any residual MCH.

2.4 Electrochemical detection

The C/M/A/A/E is produced by adding 5 µL of CA125 solution to the M/A/A/E and incubating at 30 °C for 2 h. Following incubation, the M/A/A/E is rinsed with PBS solution to eliminate excess of CA125 (denoted as C/M/A/A/E). The C/M/A/A/E is then positioned in 10 mL of 10 mM $[Fe(CN)_6]^{3-/4-}$ detection solution. Electrochemical impedance spectroscopy (EIS) is employed for determination, with a frequency range and amplitude of 100 kHz to 0.1 Hz and 5.0 mV, respectively.

3 Results and discussion

SEM was employed to characterize the surface structure of both SPE and A/E, with the findings presented in Fig. 1. Figure 1A reveals that the SPE surface exhibits a relatively even, flake-like distribution, aligning with the typical surface morphology of graphene. Upon the electrodeposition of AuNPs onto the graphene surface [21], a substantial quantity of uniform particles emerged on the electrode surface (Fig. 1B), signifying the successful deposition of AuNPs onto the SPE surface.

Figure 2 presents the EIS of SPE and A/E with varying CV scans. It is evident that the electron transfer resistance (ETR) of $[Fe(CN_6]^{3-/4-}$ on the SPE is comparatively high. This high resistance can be attributed to the limited conductivity of the unmodified SPE surface, which impacts the sensor's sensitivity. Following the deposition of AuNPs, the ETR of the A/E surface progressively diminishes as the number of deposition cycles increases from 2 to 5. The reduction in ETR upon AuNP deposition signifies an improvement in electron transfer at the electrode surface, which enhances the sensor's sensitivity. The AuNPs also contribute to the sensor's selectivity, as they provide a high density of active sites for specific binding with the CA125 antigen [22]. This can be attributed to the high electron density and exceptional dielectric properties of AuNPs, which facilitate electron transfer and enhance

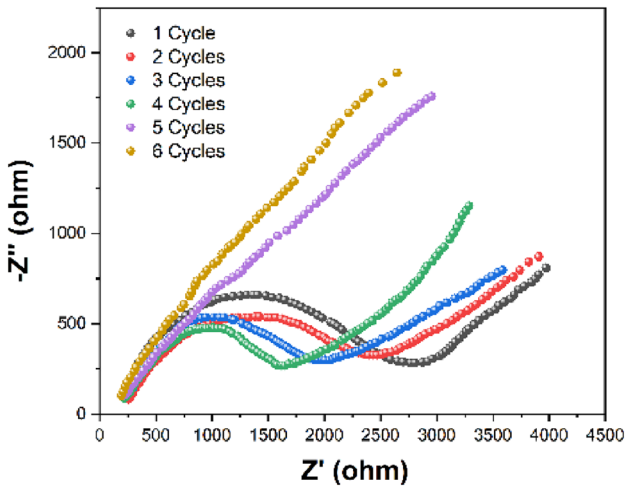

Fig. 2 EIS plots of SPE and A/E after 0–6 CV scans

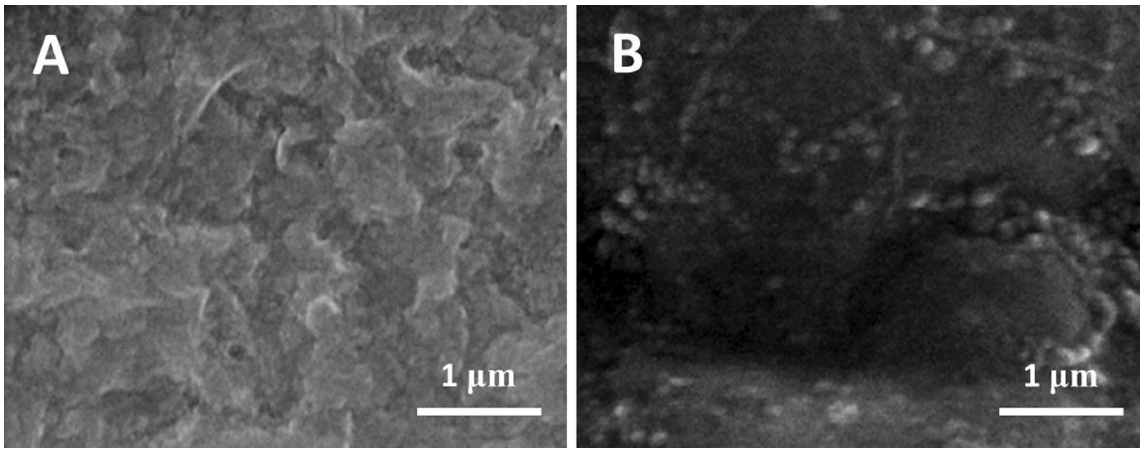

Fig. 1 SEM characterizations of SPE and A/E

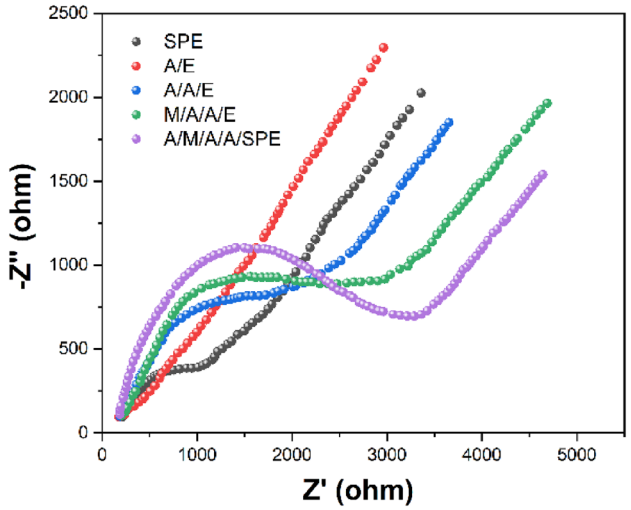

Fig. 3 EIS plots of SPE, A/E, A/A/E, M/A/A/E, and A/M/A/A/SPE in 5 mM $[Fe(CN)_6]^{3-/4-}$

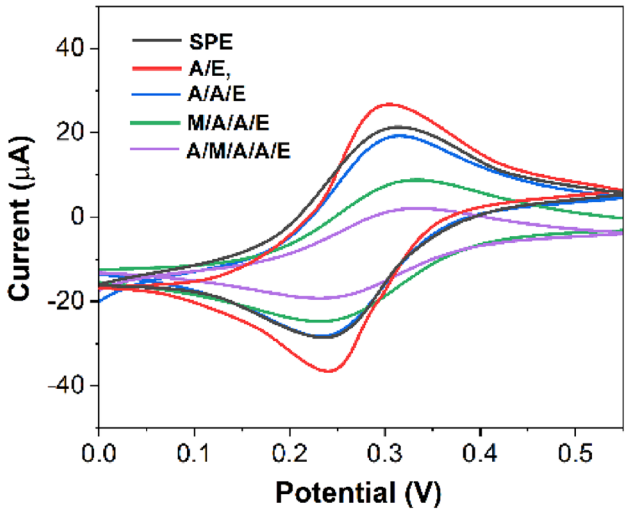

Fig. 4 CV curves of SPE, A/E, A/A/E, M/A/A/E, and A/M/A/A/E in 5 mM $[Fe(CN)_6]^{3-/4-}$

the reversibility of $[Fe(CN_6]^{3-/4}$ on the A/E surface [23]. When deposition cycles continues to rise, the ETR of $[Fe(CN)_6]^{3-/4-}$ on the A/E remains nearly constant, suggesting that the quantity of AuNPs deposited on the SPE surface has essentially reached saturation [24, 25].

We subsequently employed EIS to characterize the fabrication of the proposed electrochemical sensor, as depicted in Fig. 3. Upon electrodeposition of AuNPs, the ETR declines. This is attributable to the outstanding electrochemical properties of AuNPs, which accelerate the electron transfer rate. As CA125-A is modified on the A/E, the ETR is increased. This occurs due to the aptamer's negatively charged phosphate backbone, which causes mutual repulsion with $[Fe(CN)_6]^{3-/4-}$ and obstructs electron transfer [26]. The ETR rises further after employing the sealing agent MCH to cover the unoccupied blank sites. When 1 ng/mL CA125 is immobilized on the A/A/E, the ETR continues to increase.

Furthermore, CV has been used for monitoring the entire assembly process, as illustrated in Fig. 4. As shown in Fig. 4, the probe demonstrates favorable reversibility on the bare SPE. An improvement of probe reversibility can be observed after the AuNPs modification. As the A/A/E carries a negatively charged phosphate backbone, it would repel the negatively charged probe and influence electron transfer rate, resulting in a smaller peak current [27]. Sealing the unoccupied blank sites on the electrode surface with MCH created a dense film on the A/A/E, which further reduced the peak current. Upon the addition of 1 ng/mL CA125, it binds to the aptamer-modified electrode, causing a conformational change in the aptamer structure and creating a steric hindrance. This obstructs the electron transfer of the probe, specifically between the electrode and the redox probe $[Fe(CN)_6]^{3-/4-}$, leading to an increased peak potential difference and a decreased peak current. After adding 10 ng/mL of CA125, the peak current persisted in decreasing.

The amount of CA125-A modified on the electrode is a critical factor influencing the detection ability, so optimizing the CA125-A concentration is necessary. Figure 5A shows the effect of the CA125-A concentration toward the Ret. As the CA125-A rises from 0.1 μM to 1 μM, the Ret progressively increases. When the CA125-A continues to rise to 30 μM, the Ret plateaus and essentially ceases to change. This suggests that all available sites on the electrode surface are occupied by CA125-A, indicating that the amount of CA125-A has reached saturation. Beyond this point, additional CA125-A molecules cannot bind to the electrode surface, and consequently, the Ret does not change significantly [28]. Consequently, a carcinoembryonic antigen aptamer concentration of 1 μM was selected for subsequent experiments.

The aptamer's immobilization time is a crucial factor affecting the aptamer sensor's performance, so optimizing the immobilization time is important [29]. Figure 5B illustrates the effect of different immobilization periods for the 1 μM CA125-A. The figure shows that the Ret gradually increases of immobilization periods from 2 to 10 h. After 10 h, the Ret plateaus and essentially ceases to change, indicating that the aptamer immobilization amount has reached saturation [30]. Thus, the chosen CA125-A immobilization time was 10 h.

The incubation time also significantly affects the performance, so investigating the binding time between the M/A/A/E and CA125 is essential. The M/A/A/E was incubated with varying durations, with the experimental results displayed in Fig. 5C. It can be observed that, as the incubation time varies between 10 and 40 min, there is a substantial

increase in ETR with increasing time. When the incubation time ranges from 40 to 60 min, there is a minor decrease in Rct. As the incubation time exceeds 60 min, Rct stabilizes. This suggests that 60 min is a more suitable time for the CA125-A to specifically bind to CA125.

After the optimizations, different concentrations of CA125 were assessed using A/M/A/A/SPE via EIS. The results are presented in Fig. 6. Figure 6A displays the EIS plots of the A/M/A/A/SPE interacting with different concentrations of CA125. As shown in Fig. 6A, the impedance value showed the lowest at blank solution, and progressively increases when various concentrations of CA125 are introduced. This can be ascribed to the CA125 binding, leading to a rise in $[Fe(CN)_6]^{3-/4-}$ electron transfer resistance. Figure 6B illustrates the relationship between ETR and CA125 concentrations. The figure reveals a strong linear correlation between the sensor and CA125 from 0.2 to 15.0 ng/mL. The limit of detection can be calculated to be 0.09 ng/mL. To contextualize our findings within the broader field, we compared the performance of our graphene-based aptasensor to previously reported methods for CA125 detection (Table 1).

Reproducibility is a crucial parameter to assess the accuracy of the devised electrochemical aptasensor. To evaluate

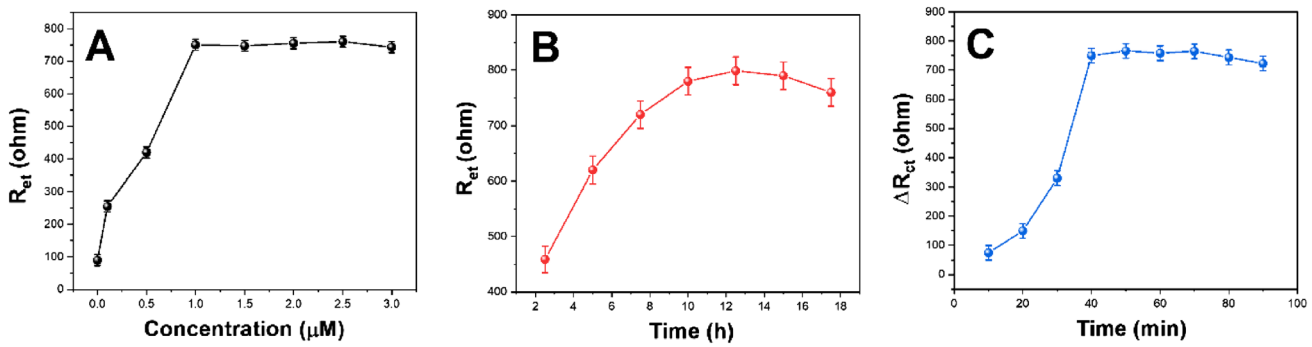

Fig. 5 The effect of **A** CA125-A concentration, **B** immobilization time, and **C** incubation time on the sensor

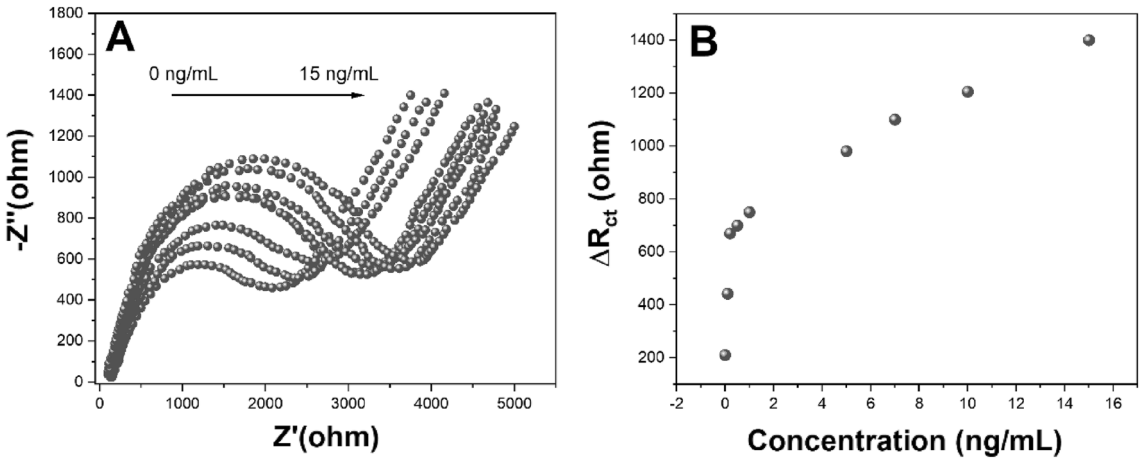

Fig. 6 **A** EIS of A/M/A/A/E toward different concentrations of CA125. **B** Plots of R_{ct} vs. CA125 concentration

Table 1 Comparison of our graphene-based aptasensor with previously reported methods for CA125 detection

Sensor	Linear range	LOD	References
MoS_2-gold-nanoflowers	0.01–50 ng/mL	0.36 pg/mL	[31]
Ag NCs/GO or Ag/Au NCs/GO	2 ng/mL–6.7 μg/mL	1.26 ng/mL	[32]
PAMAM-dendrimer/Au NPs	0.5 fg/mL	1 fg/mL–1 ng/mL	[33]
Ag_2S QDs	0.1–106 ng/mL	0.07 ng/mL	[34]
A/M/A/A/E	0.2–15.0 ng/mL	0.09 ng/mL	This work

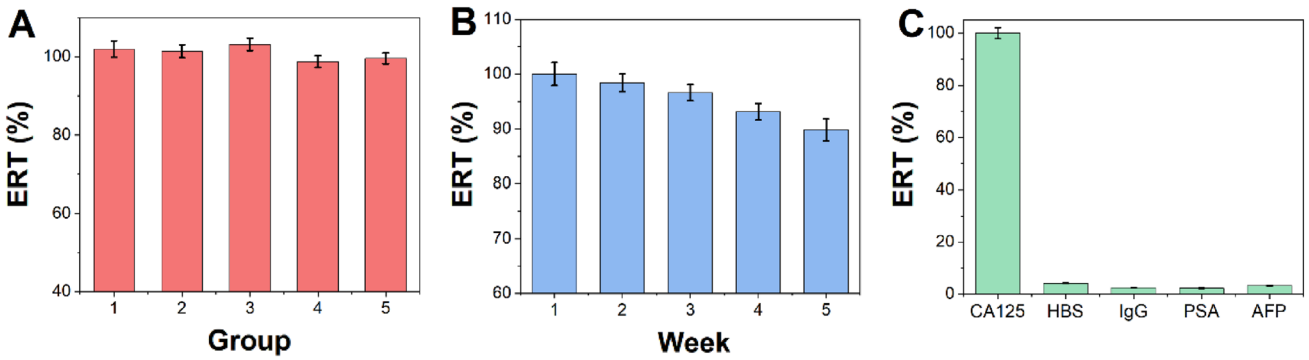

Fig. 7 **A** Reproducibility, **B** stability, and **C** specificity of the proposed A/M/A/A/E

this, five sets of aptasensors, each containing five sensors, were prepared to detect CA125 concentrations of 0.2 ng/mL, 0.5 ng/mL, 1 ng/mL, 5 ng/mL, and 10 ng/mL. Under optimal conditions, the aptasensor was assessed using an i–t curve. Figure 7A displays the ETR obtained from testing the ten sets of A/M/A/A/E, yielding relative RSD of 2.67%, 2.44%, 1.78%, 2.55%, and 3.06%, respectively. These performances indicate that the devised A/M/A/A/E exhibits strong reproducibility.

The stability of the aptasensor is evaluated by repetition of measurements of A/M/A/A/E. Ten aptasensors were prepared for determination of 1 ng/mL CA125. As shown in Fig. 7B, the fabricated aptasensor changed only 3.55% after 2 weeks and 7.03% after 3 weeks. The ETR decreased by 10.01% after 5 weeks. The decrease in ETR may be due to the accumulation or gradual inactivation of biomolecules.

Figure 7C shows the interference performance of the fabricated A/M/A/A/E toward CA125 and other interference species of AFP, HBS, PSA and IgG. As shown in Fig. 7C, all interference species can change the ETR less than 5%, suggesting that the fabricated A/M/A/A/E has excellent selectivity and specificity.

4 Conclusion

In conclusion, we successfully developed a highly sensitive and selective graphene-based aptasensor for the detection of the lung cancer biomarker CA125. Our experimental results demonstrated the aptasensor's high specificity, with a strong linear correlation between the sensor and CA125 concentrations ranging from 0.2 to 15.0 ng/mL, and a detection limit of 0.085 ng/mL. Importantly, the aptasensor exhibited excellent reproducibility, with RSD ranging from 1.78% to 3.06% for various CA125 concentrations. The sensor also demonstrated great stability, with a minor change in ETR after 5 weeks. Moreover, the sensor displayed exceptional selectivity, with interference species causing less than a 5% change in ETR. By employing a chemical reduction method for graphene synthesis and utilizing surface modification techniques, we improved the hydrophilicity and stability of the aptasensor, leading to its exceptional performance in CA125 detection.

Author contributions SJ and CJ contributed to conceptualization and writing—review and editing; JC and LY were responsible for software; JC and WX performed validation and data curation; JC did formal analysis; TL performed investigation and visualization; SJ was responsible for resources; JC, LY, and WX were involved in writing—original draft preparation; CJ was involved in supervision and project administration. All the authors have read and agreed to the published version of the manuscript.

Funding None.

Data availability The data that support the findings of this study are available on request from the corresponding author upon reasonable request.

Declarations

Conflict of interest The authors state that there is no conflict of interest. On behalf of all authors, the corresponding author states that there is no conflict of interest.

References

1. Khalid MAU, Kim YS, Ali M, Lee BG, Cho Y-J, Choi KH (2020) A lung cancer-on-chip platform with integrated biosensors for physiological monitoring and toxicity assessment. Biochem Eng J 155:107469
2. Kovalska E, Lesongeur P, Hogan B, Baldycheva A (2019) Multilayer graphene as a selective detector for future lung cancer biosensing platforms. Nanoscale 11:2476–2483
3. Ramanathan S, Gopinath SC, Arshad MM, Poopalan P (2019) Multidimensional (0D–3D) nanostructures for lung cancer biomarker analysis: comprehensive assessment on current diagnostics. Biosens Bioelectron 141:111434
4. Liu J, Wang Y, Liu X, Yuan Q, Zhang Y, Li Y (2019) Novel molecularly imprinted polymer (MIP) multiple sensors for

endogenous redox couples determination and their applications in lung cancer diagnosis. Talanta 199:573–580
5. Li W, Jia Z, Xie D, Chen K, Cui J, Liu H (2020) Recognizing lung cancer using a homemade e-nose: a comprehensive study. Comput Biol Med 120:103706
6. Yu L, Cui X, Li H, Lu J, Kang Q, Shen D (2019) A ratiometric electrochemical sensor for multiplex detection of cancer biomarkers using bismuth as an internal reference and metal sulfide nanoparticles as signal tags. Analyst 144:4073–4080
7. Biswas S, Lan Q, Xie Y, Sun X, Wang Y (2021) Label-free electrochemical immunosensor for ultrasensitive detection of carbohydrate antigen 125 based on antibody-immobilized biocompatible MOF-808/CNT. ACS Appl Mater Interfaces 13:3295–3302
8. Rebelo TS, Costa R, Brandão AT, Silva AF, Sales MGF, Pereira CM (2019) Molecularly imprinted polymer SPE sensor for analysis of CA-125 on serum. Anal Chim Acta 1082:126–135
9. Attia M, Ali K, El-Kemary M, Darwish W (2019) Phthalocyanine-doped polystyrene fluorescent nanocomposite as a highly selective biosensor for quantitative determination of cancer antigen 125. Talanta 201:185–193
10. Charkhchi P, Cybulski C, Gronwald J, Wong FO, Narod SA, Akbari MR (2020) CA125 and ovarian cancer: a comprehensive review. Cancers 12:3730
11. Wang X, Wang M, Feng L, Song J, Dong X, Xiao T, Cheng S (2022) Four-protein model for predicting prognostic risk of lung cancer. Front Med 16:618–626
12. Njoku K, Barr CE, Sutton CJ, Crosbie EJ (2022) Urine CA125 and HE4 for the triage of symptomatic women with suspected endometrial cancer. Cancers 14:3306
13. Foroozandeh A, Abdouss M, SalarAmoli H, Pourmadadi M, Yazdian F (2023) An electrochemical aptasensor based on g-C3N4/Fe3O4/PANI nanocomposite applying cancer antigen_125 biomarkers detection. Process Biochem 127:82–91
14. Zhang F, Fan L, Liu Z, Han Y, Guo Y (2022) A label-free electrochemical aptasensor for the detection of cancer antigen 125 based on nickel hexacyanoferrate nanocubes/polydopamine functionalized graphene. J Electroanal Chem 918:116424
15. Ni Y, Ouyang H, Yu L, Ling C, Zhu Z, He A, Liu R (2022) Label-free electrochemical aptasensor based on magnetic α-Fe2O3/Fe3O4 heterogeneous hollow nanorods for the detection of cancer antigen 125. Bioelectrochemistry 148:108255
16. Chen M, Han R, Wang W, Li Y, Luo X (2021) Antifouling aptasensor based on self-assembled loop-closed peptides with enhanced stability for CA125 assay in complex biofluids. Anal Chem 93:13555–13563
17. Pourmadadi M, Moammeri A, Shamsabadipour A, Moghaddam YF, Rahdar A, Pandey S (2023) Application of various optical and electrochemical nanobiosensors for detecting cancer antigen 125 (CA-125): a review. Biosensors 13:99
18. Wang Q, Zhao F, Yang Q, Wu W (2021) Graphene oxide quantum dots based nanotree illuminates AFB1: dual signal amplified aptasensor detection AFB1. Sens Actuators B Chem 345:130387
19. Fan Y, Shi S, Ma J, Guo Y (2022) Smartphone-based electrochemical system with multi-walled carbon nanotubes/thionine/gold nanoparticles modified screen-printed immunosensor for cancer antigen 125 detection. Microchem J 174:107044
20. Bharti A, Rana S, Dahiya D, Agnihotri N, Prabhakar N (2020) An electrochemical aptasensor for analysis of MUC1 using gold platinum bimetallic nanoparticles deposited carboxylated graphene oxide. Anal Chim Acta 1097:186–195
21. Ahmadi A, Khoshfetrat SM, Kabiri S, Fotouhi L, Dorraji PS, Omidfar K (2021) Impedimetric paper-based enzymatic biosensor using electrospun cellulose acetate nanofiber and reduced graphene oxide for detection of glucose from whole blood. IEEE Sens J 21:9210–9217
22. Bao Y, Ye S, Zhou C, Chen L (2022) Molybdenum (IV) sulfide nanosheet-based aptasensor for the label-free determination of bisphenol A (BPA) by electrochemical impedance spectroscopy (EIS). Anal Lett 55:1971–1979
23. AmouzadehTabrizi M, Acedo P (2022) An electrochemical impedance spectroscopy-based aptasensor for the determination of SARS-CoV-2-RBD using a carbon nanofiber–gold nanocomposite modified screen-printed electrode. Biosensors 12:142
24. Ahmadi SF, Hojjatoleslamy M, Kiani H, Molavi H (2022) Monitoring of Aflatoxin M1 in milk using a novel electrochemical aptasensor based on reduced graphene oxide and gold nanoparticles. Food Chem 373:131321
25. Jalalvand AR (2019) Fabrication of a novel and ultrasensitive label-free electrochemical aptasensor for detection of biomarker prostate specific antigen. Int J Biol Macromol 126:1065–1073
26. Hosseinzadeh L, Mazloum-Ardakani M (2020) Advances in aptasensor technology. Adv Clin Chem 99:237–279
27. Lu Q, Liu X, Hou J, Yuan Q, Li Y, Chen S (2020) Selection of aptamers specific for DEHP based on ssDNA library immobilized SELEX and development of electrochemical impedance spectroscopy aptasensor. Molecules 25:747
28. Hou Y, Long N, Jia B, Liao X, Yang M, Fu L, Zhou L, Sheng P, Kong W (2022) Development of a label-free electrochemical aptasensor for ultrasensitive detection of ochratoxin A. Food Control 135:108833
29. Tao D, Shui B, Gu Y, Cheng J, Zhang W, Jaffrezic-Renault N, Song S, Guo Z (2019) Development of a label-free electrochemical aptasensor for the detection of Tau381 and its preliminary application in AD and non-AD patients' sera. Biosensors 9:84
30. Yen Y-K, Chao C-H, Yeh Y-S (2020) A graphene-PEDOT: PSS modified paper-based aptasensor for electrochemical impedance spectroscopy detection of tumor marker. Sensors 20:1372
31. Wang X, Deng W, Shen L, Yan M, Yu J (2016) A 3D electrochemical immunodevice based on an Au paper electrode and using Au nanoflowers for amplification. New J Chem 40:2835–2842
32. Gedi V, Song CK, Kim GB, Lee JO, Oh E, Shin BS, Jung M, Shim J, Lee H, Kim Y-P (2018) Sensitive on-chip detection of cancer antigen 125 using a DNA aptamer/carbon nanotube network platform. Sens Actuators B Chem 256:89–97
33. Hamd-Ghadareh S, Salimi A, Fathi F, Bahrami S (2017) An amplified comparative fluorescence resonance energy transfer immunosensing of CA125 tumor marker and ovarian cancer cells using green and economic carbon dots for bio-applications in labeling, imaging and sensing. Biosens Bioelectron 96:308–316
34. Jin H, Gui R, Gong J, Huang W (2017) Aptamer and 5-fluorouracil dual-loading Ag2S quantum dots used as a sensitive label-free probe for near-infrared photoluminescence turn-on detection of CA125 antigen. Biosens Bioelectron 92:378–384